THIN VEILS STRATEGICALLY INTERLEAVED TO REDUCE LOW VELOCITY DAMAGES ON CFRP

L. Amorim*, A. Santos, J. P. Nunes and J. C. Viana

* IPC/i3N, University of Minho, Guimarães, Portugal
e-mail: luis.amorim@dep.uminho.pt ; web page: www.dep.uminho.pt

Key words: CFRP, Advanced composites, Thin veils, Low velocity impact, Damage.

ABSTRACT

Low velocity impact (LVI) events on carbon fibre reinforced polymers (CFRP) are one of the most problematic issues in composite applications for advanced markets, such as aeronautic, aerospace and army. Due to their own brittleness and layer-by-layer nature, when exposed to LVI solicitations, composites tend to develop internal damages that may be barely visible at naked eye. The high complex field of internal stresses developed in composite laminates during impact usually causes crack initiation and defects between layers, which may propagate (delamination) due to the low toughness that this unreinforced resin rich region exhibits. In this work, to try minimizing this propagation problem, thin veils of different materials (glass, carbon, aramid and polyester), were interleaved between different layers of a carbon/epoxy laminate typically used to produce aircraft components. In addition, to decide between which layers could be better interleave the above referred veils a theoretical study was carried out to evaluate the stresses distribution across laminate thickness when a bending moment is applied, on a carbon/epoxy laminate under study. The new carbon/epoxy laminates using the thin interleaved veils were produced by vacuum bag infusion and their mechanical characteristics and LVI responses compared with those obtained on a non-interleaved one produced in the same processing conditions. Interlaminar shear strength (ILSS) and LVI tests at four different energy impact levels were performed in order to evaluate the respective characteristics of the laminates, their damage tolerance and impact response. All laminates studied were also observed under scanning electron microscopes (SEM) for assessing their processing quality.

1. Introduction

In the last decades, due to their excellent properties, the polymeric composite materials have increasingly been used worldwide in highly demanding markets, such as, the aeronautical, aerospace and sports ones [1, 2]. Their outstanding stiffness and strength allied to a low density make them much more competitive and attractive for advanced applications than other most common traditional materials [3]. However, these materials still present some weakness when submitted to some kinds of loading, such as, impact, dynamic and flexural, due to their brittleness and layer-by-layer inherent nature [4]. Low velocity impacts (LVI) are one of the most dangerous events that composite laminate must face in their life time. These solicitations may develop imperceptible internal laminate damages, namely delaminations, that tend of propagate in service and compromise performance of composite parts [5].

Interleaving thin veils between plies have already shown to increase interlaminar fracture toughness in Mode I and II [6, 7], but there are not yet many studies carried out to demonstrate

that their usage may improve damage tolerance caused by impact events. Walker et al. [8] interleaved short fibres of different materials between each interlaminar region of a CFRP and reported a reduction of the global and local damage of these composites when compared to the non-interleaved ones. Hogg [9] has shown that interleave carbon-polyester veils, increase the impact resistance of laminates by compression after impact (CAI). Stanley et al. [10] found out that the use of polyamide (PA) veils reduced damage area and increase CAI resistance, although some void spots remained into carbon layers because the high permeability of the veil plies prevented the resin impregnation of less permeable areas. Tanoglo et al. [11], also interleaved PA veils into a CFRP laminate and has shown that those interlaminar structures improved the Charpy impact strength, despite a reduction of mechanical properties have been reported. García-Rodríguez et al. [12] introduced a low melt temperature 4 g/m2 weight coPA between each single interlaminar region and found out that, in some cases, this allowed to increase the CAI strength and reduce low velocity impact damage area in more than 100 %.

The major drawback regarding the interleave of tougher structures between the composite layers is the increase of thickness caused on the final part. Thus, in order to minimise the number of thin veils to be used, a theoretical study has been carried out in this work to evaluate the level of stresses developed across the laminate thickness in bending and, only apply the intended veils between layers where higher discrepancies between stresses had occurred.

2. Approach

In this work, only six plies of four different thin veil were used to improve the impact damage tolerance of a carbon/epoxy laminate typically used in aircraft parts to avoid thickness and weight overages.

As low velocity impact is supposed to be predominantly dominated by bending and shear stresses a theoretical study using the Classic Lamination Theory (CLT) was carried out to calculate the distribution of stresses across the thickness of the carbon/epoxide laminate studied. Then, six interfaces presenting higher difference stresses between plies were selected to interleave thin veils made from the four different materials (glass, carbon, aramid and polyester) to try achieving better LVI damage tolerance. A schematic representation of this approach may be seen on Figure 1.

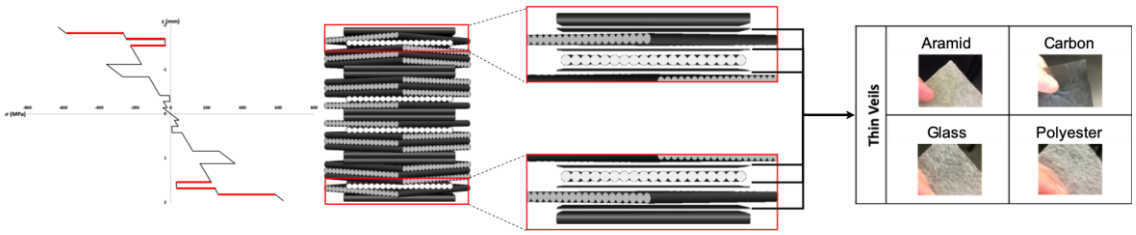

Figure 1. Approach schematic diagram

3. Experimental

3.1. Materials and processing

All CFRP laminates were produced by vacuum bag infusion using 150 g/m^2 unidirectional (UD) carbon fibre fabrics (Dynanotex HS 24/150 DLN2) provided from G. ANGELONI s.r.l.,

Italy, with a corresponding thickness of aprox. 0.145 mm, and a bi-component epoxy resin from Sika® (Biresin® CR83 epoxy resin and Biresin® CH83-6 hardener).

In order to improve impact damage tolerance of the standard laminate (LS) of reference, four unwoven thin veils made from glass (~17 g/m^2), carbon (~17 g/m^2), aramid (~14 g/m^2) and polyester (~17 g/m^2) fibres, with a thickness of 0.127, 0.14, 0.132 and 0.119 (mm), respectively, provided from ACP Composites, USA, were used as interlaminar tougher. All values present on this description were extracted from supplier materials data sheets.

Table 1 presents the lay-up used to produce the so-called aircraft standard laminate (LS) of reference i in its first line.

Table 1. Laminates stacking sequence

Laminate	Veil Type	Nº layers		Stacking Sequence
		UD Carbon tissue	Veil	
LS	-	28	-	$[0/45/90/-45/45/-45/0]_{2S}$
GL_P	Glass fibre	28	6	$[0/G/45/G/90/G/-45/45/-45/0/0/-45/45/-45/90/45/0]_S$
CL_P	Carbon fibre	28	6	$[0/C/45/C/90/C/-45/45/-45/0/0/-45/45/-45/90/45/0]_S$
AL_P	Aramid fibre	28	6	$[0/A/45/A/90/A/-45/45/-45/0/0/-45/45/-45/90/45/0]_S$
PL_P	Polyester fibre	28	6	$[0/P/45/P/90/P/-45/45/-45/0/0/-45/45/-45/90/45/0]_S$

Table 1 also shows the lay-up of the four new laminates that were produced with six plies of each type of the four above described thin veils, strategically interleaved between the previously selected layers, for being compared to the conventional one (LS) manufactured with the same stacking sequence. The capital letters G, C, A and P designates the glass, carbon, aramid and polyester veils, respectively.

All UD carbon fibre tissues and veils were first cut and, then, carefully manually placed layer-by-layer for building the laminates that were manufactured by vacuum bag infusion at room temperature and submitted to a post-curing treatment at 70 ºC, inside an oven during 8 hours. The final composite laminated plates were produced with dimensions of 650x500 (mm) and thickness of approximately 4 mm, being this latter measure slightly dependent from the type of thin veil used.

3.2. Testing

3.2.1. Laminates characterisation

A calliper rule was used to measure the dimensions in each laminate and determine the increment of thickness caused by the incorporation of the veils.

In order to evaluate the process quality, fibre orientation, void content and layer thicknesses, four samples were also randomly picked from each laminate plate and carefully polished for being inspected under the scanning electron microscope (SEM).

3.2.2. Interlaminar shear strength (ILSS) tests

Interlaminar shear strength tests were performed in accordance with ISO 14130 standard. The results allow to evaluate and compare how the different interleaved veils influence the interlaminar shear strength and failure mode. All experiments were performed using a 50 kN Shimadzu universal testing machine at a loading speed of 1 mm/min. Specimens with dimensions of 40 ×20 (mm), which means having approximately a length and a width, respectively, 10 and 5 times higher than its thickness, were used in the tests according standard recommendations.

The interlaminar shear strength of each specimen, τ, was calculated from the obtained data, as:

$$\tau = \frac{3}{4} \times \frac{F}{bh} \quad (1)$$

where, F, b, and h are the maximum applied load and the specimen width and thickness, respectively.

3.2.3. Low velocity impact (LVI) tests

A drop weight impact testing machine "Fractovis Plus" from Ceast using an anti-rebounding system was used to perform the LVI tests in all laminates. A 20 mm diameter piezoelectric hemispherical steel sticker impactor with a total drop mass of 5.045 Kg was used in the impact tests made at the energy levels of 13.5, 25 and 40 (J), while a drop mass of 16.044 Kg was used in the same impactor in the tests made at 80 J energy level. The different energy levels were obtained by carefully adjusting the impactor height between the impactor striker and specimen upper impact surface. Specimens with 150 mm of length and 100 mm of width (in accordance with ASTM D7136/D7136M standards) were held to a support steel plate by the means of four clamps with rubber tips. This supporting plate exhibits a 125x75 (mm) hole at its centre, which by staying below the specimen allows exposing it to the impact. Three specimens of each laminate were submitted to the four different impact energy levels, although only two of LS laminate had been used in the tests at the 13.5, 25, 40 (J).

The load and time were recorded by the equipment software during each impact test. Admitting a perfect contact between the impactor and the specimen, the support plate and the specimen, the specimen and clamps and by considering that kinetic energy (*KE*) equals the previously selected total energy test level, the initial velocity of the impactor (v_i) may be calculated at moment of impact from the following equation:

$$KE = \frac{1}{2} \times m{v_i}^2 \quad (2)$$

where m is the total drop mass and v_i is the initial impactor velocity.

Furthermore, during the impact, the velocity of the impactor may be calculated at any time t by using the numerical integration of the force versus time stated by the equation:

$$v(t) = v_i + gt - \int_o^t \frac{F(t)}{m} dt \quad (3)$$

where $v(t)$ is the impactor velocity at time t, g the gravitational acceleration and $F(t)$ the load measured at the same instant t. Finally, the energy absorbed by the specimen at each instant, $E_a(t)$ is determined as:

$$E_a(t) = E_{a\,i-1} + \frac{m(v_i^2 - v(t)^2)}{2} \quad (4)$$

It's well-known that the impact response depends on many factors, such as, the laminate architecture, specimen dimensions and material, impactor geometry and impact energy, being just only expected that identical specimens present similar behaviour when submitted to the same impact testing conditions and energy loading level.

In order to analyse the damage propagation onset, the simultaneous interpretation of contact load and absorbed energy histories obtained from the testing curves could be more explicit to assess laminates onset critical load (P_{cr}) and absorbed energy (E_{cr}). In this work these two critical values will be analysed concerning tolerance to damage propagation onset of each of the produced laminates at the four different impact energy levels. Figure 2 shows typical contact load and absorbed energy curves obtained from an impact test made on a composite specimen, being the critical and maximum obtained forces, P_{cr} and P_{max}, respectively, and the critical and maximum absorbed energy, E_{cr} and E_{max}, respectively identified on them.

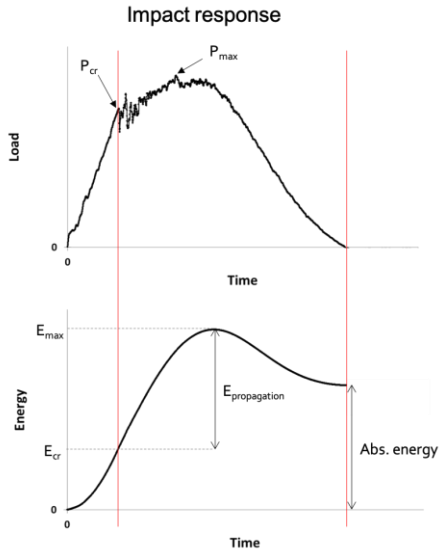

Figure 2. Curves of force and absorbed energy vs time obtained from a typical impact test made on a composite material.

Although, is important to be always aware that short time onset phenomena may be induced by simultaneous and diverse energy dissipater mechanisms that may be mismatched during the impact history analysis

4. Results and discussion

4.1. Laminate characteristics

In order to evaluate the increment of thickness due to veils incorporation, four measurements were made in each laminate impact specimen. Laminate thicknesses and their increment due to the use of interleaved thin veils may be compared with the non-interleaved one from the results presented in Table ***2***.

Table 2. Laminates thickness

Laminate	Thickness (mm)		Thickness increment (%)
	Average	Std. Dev.	
LS	3.86	0.055	-
GL_P	4.32	0.031	12.0
CL_P	4.77	0.341	23.5
AL_P	4.55	0.023	17.7
PL_P	4.42	0.021	14.5

As expected, in accordance with the data sheets supplied by the veils manufacturer the laminates interleaved with carbon veils (CL_P) presented higher thickness, followed by the one using interleaved aramid veils (AL_P) and, the laminates reinforced with polyester veils (PL_P) revealed to have slightly higher those having glass fibre veils.

Figure 3 shows scanning electron microscopy (SEM) images that were used to evaluate the laminate structures, veils lamina thicknesses and presence of void spots. Highlighted in red, it's possible to see the interleaved veils in the figure. These visualizations have also shown that, in contrast of the other veils, polyester fibres on PL_P laminate apparently lost their typical circular section during the infusion process and present an irregular cross section in the final composite plate. The dark spots on images represent the adhesive resin used to bond and keep together the carbon fibres and the weft thread in the UD tissue.

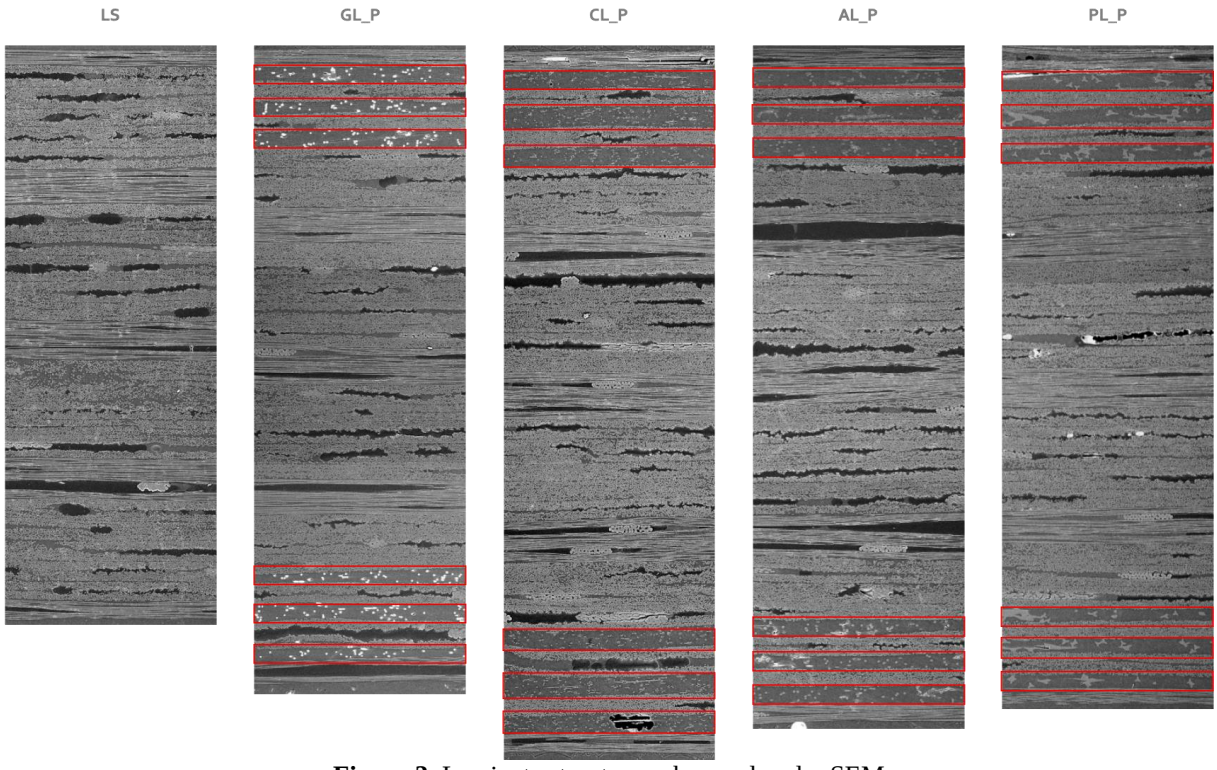

Figure 3. Laminate structures observed under SEM

Figure 4's bar chart shows the average thickness determined from the values obtained from each veil lamina on the four interleaved laminates. As may be seen, the measurements done by SEM have shown that the thicknesses of all veils followed the tendency presented in their supplier data sheets, although all of them demonstrated to be slightly thinners than migth be expected from those data.

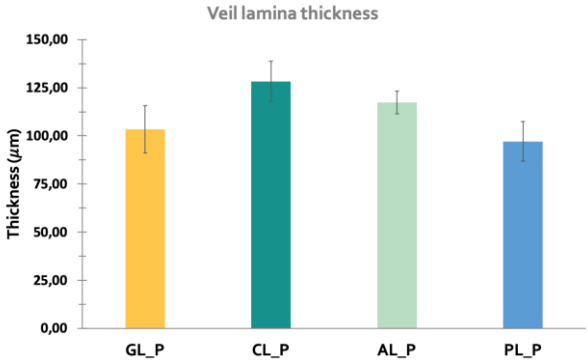

Figure 4. Veils lamina thicknesses obtained from SEM observations

SEM observations were also used to inspect the presence voids in the laminates after processing. As may be seen in Figure 5, all interleaved laminates have presented some void spots. The observations have shown that CL_P and AL_P laminates presented higher amount of voids than the other interleaved ones and that they were typically found in the first and second laminae near their surfaces. On the other hand, smaller void spots were typically found mostly in the UD carbon fibre laminae of the GL_P and PL_P laminates. LS laminate, that was previously inspected in other work that will be published soon, does not show to has presence of voids spots.

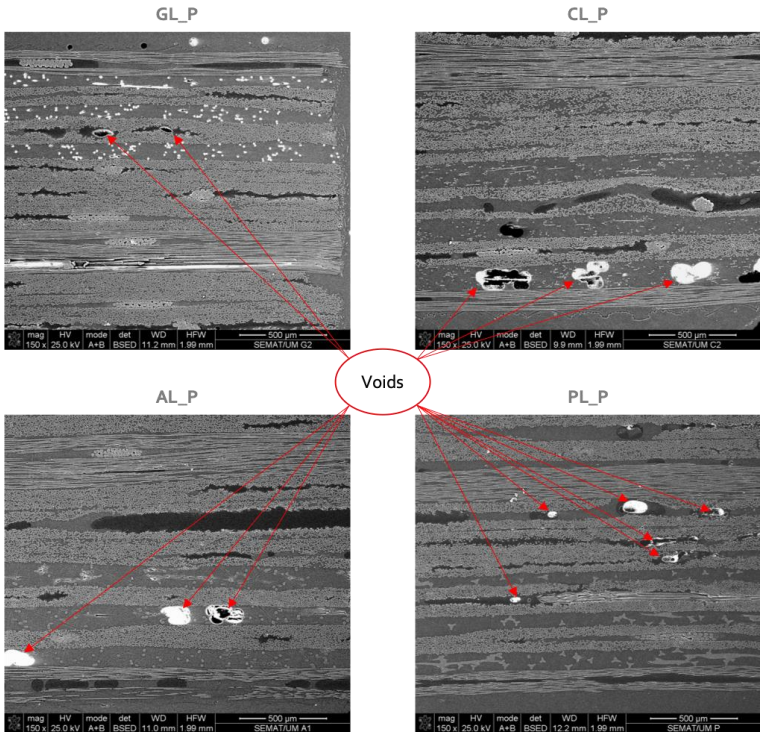

Figure 5. Voids spots on interleaved laminates.

As it was expected, the inclusion of veils caused and increment on laminate thicknesses. By promoting an easy resin flow during vacuum bag infusion process, veil layers lead to higher resin concentrations than UD carbon fibre ones and this increases the laminate thickness. The SEM observations also appeared to suggest that, during the curing process, the epoxy resin reached a high enough exothermic peak temperature to melt the polyester fibres on PL_P

laminate which may have cause the changing of initial circular shape of their to a much irregular one.

4.2. Interlaminar shear strength (ILSS)

Figure 6 presents the interlaminar shear strength results obtained from the ILSS tests made on laminates.

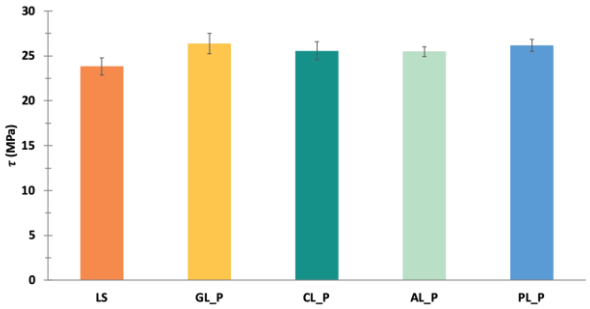

Figure 6. Interlaminar shear strength test results.

As it may be observed, all interleaved laminates presented higher global resistance to delamination in comparison to non-interleaved one. It seems that the inclusion of thin veils led to a more uniform distribution of shear stresses on the selected interfaces, redirecting the loading to the carbon fibre tissues and increase by that way the interlaminar shear resistance. Future work will be carried out in order to observe the typical failure mode of each laminate under optical microscopy.

4.3. Low velocity impact (LVI)

As mentioned above, the P_{cr} load value is an important characteristic to allow analyse the damage propagation onset. Figure 7 shows the average P_{cr} values obtained for each laminate from the impact tests performed at 13.5, 25, 40 and 80 (J) energy levels.

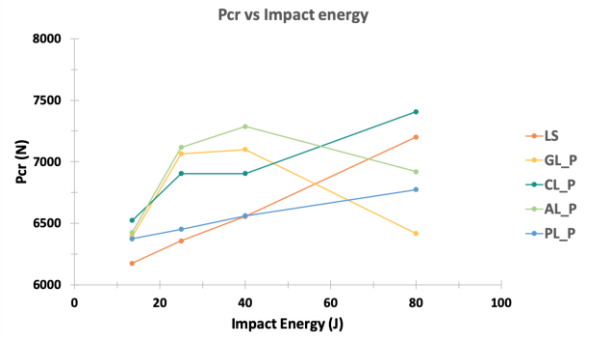

Figure 7. Laminates P_{cr} analysis at different impact energy levels.

As it may be seen, up to 40 J of impact energy level, all interleaved laminates presented higher P_{cr} values in comparison to the LS laminate, while at 80 J only CL_P has shown to be able to present higher P_{cr} load than the LS one before damage propagation onset. Moreover, all

laminates have shown an increase on P_{cr} with the increment of impact energy, with the exception of GL_P and AL_P laminates, that presented lower P_{cr} values at 80 J than those ones observed at 25 J.

It is possible to concluded that the CL_P laminate presented the better performance at 13.5 J of impact energy level. However, when the impact energy level rises until 40 (J), the AL_P laminate have shown better ability to bear load before damage propagation, followed by the GL_P laminate and, after, the CL_P one. The PL_P laminate demonstrated the poorest behaviour in all the three lower impact energy levels.

Finally, at 80 J impact energy level, both AL_P and GL_P presented a drastic reduction on their capability to bear load before damage propagation. In the first case, lower values than those reported at 25 J were observed, and in latter case, there were obtained similar values to those achieved at 13.5 J impact energy level. At 80 J, all other laminates presented higher P_{cr} values than those that were obtained at 40 J. The better performance was obtained in the CL_P laminate in these conditions, which was followed by the LS, AL_P, PL_P and GL_P laminates, respectively.

Another way to evaluate the ability to bear load before damage propagation may be obtained by analysing the ratio between P_{cr} and the maximum load that the laminate can bear (P_{max}). If this ratio is close to 1, it means that the laminate can bear almost the entire load without damage propagation and, on the other hand, the lower this ratio is the lower seems to be the laminate resistance to absorb the impact loading without suffering severe damage. Figure 8 presents the evolution of this ratio for each laminate at each impact energy testing level.

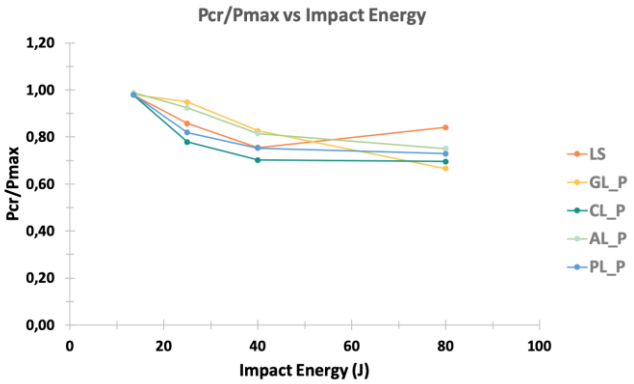

Figure 8. Ratio between P_{cr} and P_{max}.

As it may be seen, all laminates presented a ratio close to 1 at 13.5 J impact energy level. When the impact energy level was increased to higher energy levels, these ratio values decreased for almost all laminates as expected and some differences were observed on their response. For the 25 and 40 (J) energy levels, the GL_P and AL_P laminates presented the better performances, followed by the LS, PL_P and, finally, the CL_P laminates, respectively. Although, when the impact energy was increased to 80 J, the P_{cr}/P_{max} ratio dropped down for the GL_P laminate, which presented the worse behaviour, in contrast to the LS laminate that has shown to have the best performance under this impact conditions.

By analysing the P_{cr} values obtained, it may concluded that until impact energy level of 40 J all laminates presented a roughly similar consistent behaviour. However at 80 J, an important decrease were observed on the performance of the AL_P and GL_P laminates, which had presented better global ability to bear load than all other laminates up to the 40 J impact energy

level. Despite the higher number of void spots found from the SEM observations made on AL_P laminate, it seems that aramid fibre veils were able to improve the resistance to damage propagation likely due to the recognised ability of these fibres to dissipate energy. In the case o GL_P laminate, it seems that the better impregnation they presented in the SEM images resulted in a more efficient toughening of the interlaminar regions selected to place the veils, which has provided higher resistance to damage propagation onset. Further analysis of load vs displacement data correlated with non-destructive and destructive tests will must be carried out to better explain the loss of performance observed in the GL_P and AL_P laminates at the 80 J impact energy level.

The laminate interleaved with carbon fibre veils has shown to have higher overall absolute values of P_{cr} than LS laminate up to the impact energy level of 40 J. However, at the higher impact energy level of 80 J, its behaviour has shown to be worse than LS laminate. One of the reasons for this behaviour may be explained by the larger thickness presents by the CL_P laminates relatively to the LS ones. On the other hand, the higher number of void spots observed under SEM on the toughened interface of CL_P laminates, may drive to the worse behaviour they presented at the 80 J impact level in relative terms.

Finally, in contrast to what was expected due to the ductile nature of polyester fibres, the PL_P laminates exhibited poorest performance until the 40 J impact energy level which may be related with the large number of voids found in the SEM observations in the intra and interlaminar untoughened regions.

Another important factor to be studied is the value of critical absorbed energy, E_{cr}, the laminate dissipated until the damage propagation onset happens. Figure 9 plots the E_{cr} average values for all laminates studied in this work at the four impact energies previously defined.

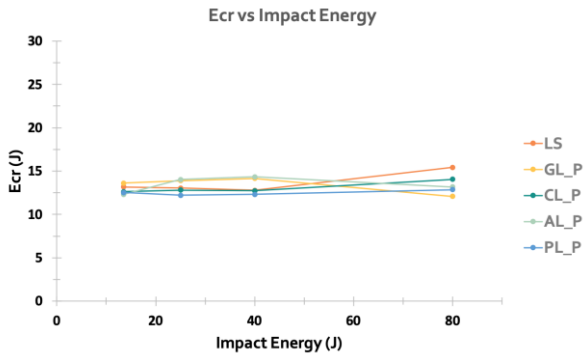

Figure 9. Laminates E_{cr} analysis at different impact energy levels.

As it may be observed on Figure 9's chart, no relevant differences were found between the laminates concerning the amount of energy absorbed before damage propagation. All laminates seemed to present an energy threshold at the damage propagation onset between 12 and 15.5 (J),. At the lower impact energy level of 13.5 J, the CL_P, AL_P and PL_P laminates presented almost the same amount of E_{cr}, while LS and GL_P laminates have shown better capability of dissipate energy before damage propagation. When the impact energy rises to 25 and 40 (J), GL_P and AL_P laminates seem to be able to dissipate slightly higher energy without severe damage than the other ones. At 80 J, LS laminate presented higher values of E_{cr} when compared to the interleaved laminates. Once again PL_P laminate presented the poorest behaviour up to the 40 J impact energy testing level, while it showed to be slightly better than GL_P laminate at 80 J.

The ratio between E_{cr} and the maximum energy absorbed be the laminates (E_{max}) may also give an idea of the amount of energy dissipated without damage propagation. When this ratio is close to 1, the higher is the amount of energy dissipated before damage propagation. Such ratio, between the values of E_{cr} and E_{max} obtained in each laminate from the impact tests made at the four energy levels are shown in Figure 10.

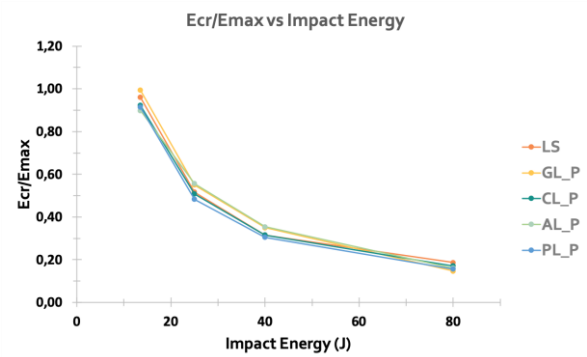

Figure 10. Ratio between E_{cr} and E_{max}.

As it may be seen in Figure 10, no big differences were observed on the ratio obtained for the different laminates at each energy impact level. At the 13.5 J impact energy level, the GL_P and LS laminates presented values much closer to 1 than the other laminates, which presented similar values among themselves. At 25 and 40 (J), GL_P and AL_P laminates presented similar and slightly better behaviour than the other laminates, which also showed almost the same results between them, being the worst performance presented by the PL_P laminate at 25 J impact energy level. Finally, at 80 J impact energy level, all interleaved laminates presented very similar performance, while LS laminate seemed to present a tiny better behaviour.

The analysis of the critical energy to onset damage propagation doesn't show a big difference between the interleaved and non-interleaved laminates. Although, as it was expected by the analysis of P_{cr} load, GL_P and AL_P laminates have shown to have better performance than all the other laminates, specially for impact energies levels between the 25 and 40 (J). The main reasons for this behaviour are probably those already mentioned before and additional experimental work, as non-destructive and destructive tests, will must be carried out in order to better evaluate the main dissipation mechanisms occurred during the impact event.

5. Conclusions

In this work, a conventional laminate used in the production of aircraft components was strategically interleaved with six layers of four different thin veils in order to improve its tolerance to impact events. The initial conventional and the new interleaved laminates were characterized and compared with respect to their thicknesses and the presence of voids after processing by vacuum bag infusion was evaluated by using the scanning electronic microscopy (SEM) technique. Their global resistance to delamination and tolerance to damage propagation were also investigated by low impact velocity (LVI) tests made at different energy levels. Vacuum bag infusion process was shown to be particularly efficient to produce the conventional non-interleaved laminates. However, when veils were interleaved between the UD carbon layers used in the laminates, an easy resin flow environment was created which had slow dawn

the impregnation of the UD carbon tissues causing dry spots (voids) inside the laminate. The strategical placement of thin veils were made between layers where larger difference of stresses due to a bending moment. The use of these thin veils revealed to improve the overall resistance to delamination, despite the voids that were detected inside the interleaved laminates during their observation under SEM. Under low velocity impact tests, glass and aramid fibre veils interleaved laminates demonstrated slight enhancements on P_{cr} and E_{cr} when compared to non-interleaved laminate, specialty for impact energies up to 40 J.

Future work will be carried out in order to obtain a better characterization of the laminates. Tensile and three-point bending tests will be performed and the failure mode of laminates under ILSS tests will be analysed. Non-destructive and destructive test will be also used to evaluate the damage area caused and understand the main mechanisms used during LVI tests to dissipate energy. A new strategical placement of the veils is also being studied to evaluate their influence when placed at the interfaces of higher shear tensions when laminate is under a bending moment.

REFERENCES

[1] M. F. S. F. Moura, A. B. Morais, and A. G. Magalhães, *Materiais Compósitos - Materiais, Fabrico e Comportamento Mecânico*, 1 ª. Porto: Publindústria, 2005.

[2] F. A. Administration, "Aviation Maintenance Technician Handbook - Airframe," *Aviat. Maint. Tech. Handb. - Airframe*, vol. 1, p. 588, 2012.

[3] G. Gardiner, "Aerocomposites: The move to multifunctionality : CompositesWorld," 2015. [Online]. Available: http://www.compositesworld.com/articles/aerocomposites-the-move-to-multifunctionality. [Accessed: 14-Jul-2017].

[4] F. Gnädinger, P. Middendorf, and B. Fox, "Interfacial shear strength studies of experimental carbon fibres, novel thermosetting polyurethane and epoxy matrices and bespoke sizing agents," *Compos. Sci. Technol.*, vol. 133, pp. 104–110, 2016.

[5] V. Tita, J. de Carvalho, and D. Vandepitte, "Failure analysis of low velocity impact on thin composite laminates: Experimental and numerical approaches," *Compos. Struct.*, vol. 83, no. 4, pp. 413–428, 2008.

[6] M. Kuwata and P. J. Hogg, "Interlaminar toughness of interleaved CFRP using non-woven veils: Part 1. Mode-I testing," *Compos. Part A Appl. Sci. Manuf.*, vol. 42, no. 10, pp. 1551–1559, 2011.

[7] M. Kuwata and P. J. Hogg, "Interlaminar toughness of interleaved CFRP using non-woven veils: Part 2. Mode-II testing," *Compos. Part A Appl. Sci. Manuf.*, vol. 42, no. 10, pp. 1560–1570, 2011.

[8] L. Walker, M. Sohn, and X. Hu, "Improving impact resistance of carbon- ® bre composites through interlaminar reinforcement," *Compos. Part A*, vol. 33, pp. 893–902, 2002.

[9] P. J. Hogg, "Toughening of thermosetting composites with thermoplastic fibres," *Mater. Sci. Eng. A*, vol. 412, pp. 97–103, 2005.

[10] N. H. Nash, T. M. Young, and W. F. Stanley, "An investigation of the damage tolerance of carbon / Benzoxazine composites with a thermoplastic toughening interlayer," *Compos. Struct.*, vol. 147, pp. 25–32, 2016.

[11] B. Beylergil, M. Tanoglo, and E. Aktas, "Effect of polyamide-6 , 6 (PA 66) nonwoven veils on the mechanical performance of carbon fi ber / epoxy composites," *Compos. Struct.*, vol. 194, no. February, pp. 21–35, 2018.

[12] S. M. García-rodríguez, J. Costa, V. Singery, I. Boada, and J. A. Mayugo, "The effect

interleaving has on thin-ply non-crimp fabric laminate impact response : X-ray tomography investigation," *Compos. Part A J.*, vol. 107, no. January, pp. 409–420, 2018.

Please sign and date this form and retain a copy for your records. Please include this page with your paper/abstract.

TERMS AND CONDITIONS

By submitting an abstract/full paper all authors agree to the below terms and conditions.

- Submitting authors must declare that the abstract/s submitted are the original work of at least one author/presenter.
- If the abstract/full paper is accepted as an oral and/or poster, at least one abstract author will register, pay and attend ICCST/12.
- Presenting authors are required to register and pay for the conference. No funding is provided to presenters.
- If the abstract/full paper is selected, consent is provided for the presentation slides (for oral presenters), video, audio recording and photos taken during the oral presentation/poster presentation to be used and published by ICCST/12 including being provided to delegates of ICCST/12.
- Submitting authors must declare the work described in the abstract/full paper has appropriate approval under local, ethical and animal experimentation rules.
- Submitting authors must declare that their work does not conflict with any existing copyright agreements with alternate publishers.

COPYRIGHT RELEASE AGREEMENT

By Submitting an abstract/full paper, the Owner/s:

- warrants that he/she is the sole creator and/or owner of all copyrights in the manuscript, and that he/she has full power to enter into this Agreement and that this Agreement does not infringe the rights of any third party.
- The Owner/s does hereby assign and transfer to ICCST/12 the following copyrights in the manuscript, without reservation or exclusion.
- The Owner agrees that the Assignee shall from here on own the said copyrights in the manuscript, to benefit and dispose of these rights in any way and at his/her sole discretion.
- The Parties agree that this Agreement shall be binding upon the legal successors and assigns.

Paper Title:	_____	
Date: 25/04/2019	Lead Author: _____	X _____ Sign